Academia
Engineering

10.20935/AcadEng8642

Research Article

I-System's stability indicators for underground and surface openings in challenging conditions

H. Bineshian[1,*]

[1] Amberg Engineering AG, Delhi, India

* Correspondence: drbineshian@ambergindia.com

Received: 23 August 2026 | **Accepted:** 8 November 2026 | **Published:** 17 November 2026

Abstract

Introduction: This article presents the outcome of a research project that developed equations for quantifying stability indicators for designers, engineers, and geologists working on underground and surface structures such as tunnels and slopes. The research is conducted as part of the Udhampur–Srinagar–Baramulla Rail Link (USBRL) project in the state of Jammu and Kashmir in India between 2018 and 2024. The developed equations include arch-action time, active span, slip-action time, size of plastic zone, deformation limits, and support system stress, which are related to the Index of Ground-Structure (I-System). The research sought to enhance the I-System's comprehensiveness and address the gap between classification, characterisation, and stability assessments to facilitate ground–structure interaction evaluation, ground behaviour identification, and associated hazard and risk diagnosis. This will also synchronise geological, geotechnical, and geomechanical assessments between the project design and execution teams, eliminating judgement dispersion, and unifying generation of a mitigation measure as an appropriate response to ground behaviour and safety assurance.

Materials and methods: To relate the stability indicators to the I-System, I-Value was selected as the primary parameter for measurement. Logical parameters were then chosen as stability indicators and related to the I-Value and other geometrical parameters. Data was collected between 2018 and 2024 during the execution of the elements of the USBRL project including tunnels T01, T05, T13, and T14 with an overall length of 46 km. The correlations between I-Value and stability parameters proposed in this paper are based on empirical and experimental principles. The research was fed by extensive experience, which contributed to generally dependable final outcome. Analytical and numerical verification is not conducted due to limitations involved with these two methods.

Results: The data pairs resulting from the surveyed, collected, and experimented data during the project's advancement and stability indicators as dependent variables produced consistent linear and non-linear regression outputs with acceptable predicted values. This reliability was proven during the excavation.

Conclusions: The outcome of the research has been successfully used in the design and construction of the tunnel projects in the USBRL in the highly challenging conditions of the Lesser Himalayas. The study is conducted in rock and soil medium with highly complex geological formations and tectonised conditions; the stability indicators proposed here may also be applicable to similar conditions, though there is scope for further research to enhance the outcomes of this study.

Keywords: active span; arch-action time; deformation limit; I-System; I-Value; plastic zone; slip-action time; slopes; support system stress; tunnelling

1. Introduction

Stability indicators such as arch-action time, active span, size of plastic zone, deformation limits, and support system stress for underground spaces and slip-action time for surface structures are key parameters in identifying ground behaviour and its associated hazards during the design phase. These parameters are also critical for engineers and geologists to enhance their understanding of ground conditions and construction management. They inform the selection of appropriate support systems, excavation methods, instrumentation strategies, preventative measures, and design optimisation during the construction phase. The application of a reliable classification and characterisation system such as the Index of Ground-Structure (I-System) [1] is an efficient method for estimating these parameters due to its comprehensive applicability for a range of materials, including rock, soil, tailing, and waste, for underground, semi-surface, and surface structures [2–6]. A brief overview of the I-System is provided in **Table 1**. The mathematical expression of the I-System is represented in **Equation (1)** [1].

$$(I) = (A_i + C_i + H_i + P_i + S_i) \times DF_i \times ET_i \quad (1)$$

where (I) is the I-System's value or I-Value, A_i is the Armature Index, C_i is the Configuration Index, H_i is the Hydro Index, P_i is the Properties Index, S_i is the Strength Index, DF_i is the Dynamic Force Impact, and ET_i is the Excavation Technique Impact.

Table 1. A brief overview of the Index of Ground-Structure (I-System).

I-Value		Descending scale of competency of ground–structure	Associated hazard/risk colour code	Hazard/risk level
Range	I-Class			
100–91	I-01	Extremely good	Green	Extremely low
90–81	I-02	Very good	Green	Very low
80–71	I-03	Good	Green	Low
70–61	I-04	Relatively good	Green	Relatively low
60–51	I-05	Average	Yellow	Average
50–41	I-06	Below average	Yellow	Above average
40–31	I-07	Relatively poor	Yellow	Relatively high
30–21	I-08	Poor	Orange	High
20–11	I-09	Very poor	Orange	Very high
10–0	I-10	Extremely poor	Red	Extremely high

Unlike most older classifications, the I-System is not based on the Rock Quality Designation (RQD) and is not a modification of any existing system. This is the first classification applicable to all varieties of geomaterials. It takes into account ground problems and structural geological configurations, the scale effect of openings, the negative impact of earthquakes, and excavation techniques.

Unlike the "Q" ranging from 1000 to 0.001 on an open logarithmic scale, which is problematic and only applicable to rocks, the I-Value meaningfully and evocatively spans 100 to 0 on a linear scale. This system classifies ground–structure interaction into ten definable classes within a limited but equal range for each (ten scores per class) from best (Extremely Good) to worst (Extremely Poor) ground, categorised as I-01 to I-10 (**Table 1**). A colour code is defined for each individual I-Class to represent the hazard and risk level associated with it. Mitigations are provided for all risk categories within the I-System's output.

The I-System generated a new field of knowledge in ground engineering by unifying soil and rock mechanics into a single, comprehensive classification and characterisation framework. Historically, ground engineering relied on separated, rock-specific empirical systems like Bieniawski's Rock Mass Rating (RMR) or Barton's Q. The I-System fundamentally changed this by introducing a holistic methodology that evaluates the mutual interaction between any type of engineering structure and the surrounding ground of any type (rock, soil, tailing, and waste).

1.1. Breaking the rock–soil binary

Traditional empirical systems are limited to rock mass and fail in mixed ground, soil–rock transitions, soil, or highly unstable, poor ground conditions. The I-System bridged this gap:

- Universal application: It applies seamlessly to all rock, soil, tailing, and waste media, whether above or below ground.
- Sector cross-compatibility: The system offers standardised engineering assessments across civil, mining, and oil and gas structures.
- Objective consistency: By relying on mathematical parameters, it reduces the subjectivity inherent in traditional geological engineering judgments.

1.2. Multi-dimensional interaction parameterisation

Instead of isolating the geology, the I-System calculates ground behaviour through a dynamic matrix of indices and real-world impact factors:

- The key indices: It integrates 20 ground characterisation and 7 design parameters, including the Armature Index (Ai), Configuration Index (Ci), Hydro Index (Hi), Properties Index (Pi), and Strength Index (Si).
- Operational impact factors: Unlike predecessor systems, it directly factors in the excavation technique (ETi) and dynamic forces (DFi) affecting the ground.
- The I-Class scale: These inputs generate a single mathematical value between 0 and 100, placing the environment into 10 highly precise competency classes from I-01 (best; Extremely Good) to I-10 (worst; Extremely Poor).

1.3. Paradigm shift from diagnosis to active support design

The I-System evolved from a simple diagnostic tool into a complete engineering method known as I-TM (I-System's Tunnelling Method). It expanded the field's knowledge base by replacing "passive observation" with "predictive engineering", switching the tunnelling methods from reactive methods to a proactive system:

- Behaviour forecasting: It outputs direct predictions of ground behaviour, stand-up time, and specific hazard risks.
- Integrated solutions: It provides immediate, correlated recommendations for support systems, excavation techniques, and safety instrumentation.
- Life-time structural verification: The methodology governs projects through a continuous loop from pre-design, structural dimensioning, and active construction to post-excavation damage assessment.

1.4. Real-world validation in an extreme environment

The true capability of this new field of knowledge was demonstrated during the breakthrough of the Udhampur–Srinagar–Baramulla Rail Link (USBRL) project in India (e.g., tunnel T01 through the treacherous Reasi Thrust of the Lesser Himalayas) [7–9]. Conventional methods completely failed in the visco-elasto-plastic, heavily saturated ground, nearly forcing the tunnel to be abandoned. Implementing the I-System allowed engineers to accurately diagnose a purely plastic ground response with near-zero arch-action time. It successfully guided the shift from standard ground consolidation to pre-excavation ground solidification, controlling enormous thrust pressures, and achieving a safe breakthrough.

1.5. Integration with modern geophysics

The system utilises geophysical parameters that can be sourced from reliable references or techniques; however, it is integrated with modern geophysical technology utility, such as Amberg Technologies' Seismic Prediction software (TSP Ease 3.0) [10] that eases the application. This allows seismic P- and S-wave velocities recorded ahead of an excavation face to be immediately translated into I-Classes, giving engineers real-time data to adjust support strategies on the fly.

This paper presents the findings of research conducted on the USBRL project, including the T01, T05, T13, and T14 tunnels [11]. These tunnels have an overall length of 46 km and were designed and supervised during construction by the author's team from 2015 to 2025 [7–9, 12, 13]. The paper establishes a correlation between stability parameters and the I-System, which was applied for these tunnels. This study presents a novel methodology for engineers and geologists to assess the stability of underground structures and slopes during design and construction, based entirely on the I-System. The rationale for selecting I-Value for this application is detailed in the present section.

Geological formations of the above-stated projects include Kharikot, Murree, Shivalik (lower), Sirban, Subathu, and Trikuta. These are located in the overcritical wedge of the Lesser Himalayas. The most significant thrust zones in which the projects are situated are the Reasi Thrust (RT) and the Main Boundary Thrust (MBT). The project zone passes through jointed and highly fractured zones with challenging mechanical behaviour, including gravity-driven, squeezing, heaving, large lateral deformation, visco-elastic–plastic, and even fully plastic responses to excavation.

2. Materials and methods

The research has employed theoretical concepts and developed empirical relationships using logging data, experiments, and experience during the construction procedure and everyday consequences at tunnelling

works over a ten-year period of construction. Given that the research aimed to relate stability indicators to the I-System, this study has been conducted following a structured approach as follows:

- Outline: The outline is defined as a scenario, situation, or condition in which the stability indicator is defined for and is applicable.
- Primary parameter: The I-Value is selected as the primary variable for the stability indicator. It represents the I-System in defining the ground–structure's competency. The I-Value is intended to be the main variable for definition of the stability indicators. Therefore, the same is measured in a regular and systematic manner in the form of face mapping (referred to as I-Logging for the measurement of the I-Value) for the research considering the relationships for each scenario.
- Logics for stability indicators: Stability indicators are defined based on theoretical concepts. Crucial geometrical parameters are chosen as variables for the stability indicators to be related to in addition to the main parameter (I-Value) as per the definition of each scenario. The geometrical parameters of the structure are the parameters, which have direct effects on the stability assessment.
- Principle method: Empirical relationships are established for the relationships between stability indicators, I-Value, and geometrical parameters. These relationships are dimensionless or have a dimension imbalance. They are defined after linear and non-linear regression analysis and engineering logics; however, the units are defined based on the observations rather than mathematical balance.
- Main materials: In situ experiments were the primary source and material for the research, which fed the regression analysis and the study overall.
- Verifying the outcome: The research's outcome was verified by extensive experience available to the team and gained during the work in extremely challenging conditions. The output provides relatively stable measures of stability indicators defined in this research based on the observations made during the project using 3D monitoring, instrumentations, and in situ measurements. Analytical and numerical verification was not conducted due to the limitations of these methods.

The research was executed by a team of engineers and geologists comprising three senior engineers, three senior geologists, a survey team, a monitoring team, and the author. The only equipment employed was the Unigrout system for Ground Conductivity Designation (GCD) measurement. Water was the only material used for injection in GCD testing (Section 3.4).

A four-stage protocol is implemented to address anomalies in recorded data for the entire study. The criteria focus on administrative (human-related) and measurement (tool-related) errors that produce global outliers—values markedly distant from the overall dataset—which may compromise model integrity. The objective was never to remove data to improve probability values, and such considerations were excluded from the process. Neither the interquartile range nor the Z-score was applied, as the natural trend of the data remained suitable. The procedure comprises 1. detection, 2. investigation, 3. documentation, and 4. removal.

Python 3.7 was used for best-fit analysis of the data. The mean absolute error (MAE) is calculated for the data range covered by the proposed empirical equations. Relative errors are computed by dividing the MAE by the mean of measured values and presented in percentage form alongside the coefficient of determination to evaluate the goodness of fit and to assess the reliability and certainty of the estimated values. The limitations of each equation are outlined together with recommendations to improve the reliability of the proposed models.

3. Results

3.1. Arch-action time—underground openings

Self-stabilisation of the roofs of civil and mining underground spaces is initiated by the development of an arch-like response of the ground to excavation or opening. This phenomenon is known as 'arch action' irrespective of the roof being considered a one- or two-way spanning slab, which is also referred to as compressive membrane action in a two-way slab. The arch-action time for underground spaces, as part of ground–structure behaviour, is defined as the maximum period between exposure of the roof by excavation and the ground's wake-up moment (the initiation of movement) due to disturbance generated by excavation works. This disturbance initiates uncontrolled and sometimes violent mechanical behaviour that is part of a failure procedure. The failure procedure concludes with a sudden occurrence known as 'collapse'.

Research undertaken between January 2020 and November 2023 examined the arch-action time for tunnel T13 during the excavation phase of the Dugga–Sawalakot project in Jammu and Kashmir, India. The scope encompassed a 9.26 km main tunnel, a parallel escape tunnel of identical length, and a station yard with an enlarged cross-section. This research provided the foundation for establishing a mathematical correlation between stability parameters and the I-Value [11]. A total of 70 data pairs of calculated I-Value and measured arch-action time were used after removing anomalies from the recorded data as per the protocol provided in Section 2. The data pairs were obtained through crack mapping procedure including measurements on crack aperture increments and length propagation, 3D monitoring data, convergence details, and observations from the glass-strip gauges. The initial sample size, prior to the exclusion of anomalies, was 76. All six anomalies were attributable solely to human error, specifically delayed or unobserved measurements recorded at the end of shifts or during shift handovers. These coincided with changes in personnel and resulted in values exceeding three times the normal threshold observed in the baseline data trend. Following detection, investigation confirmed this cause; the findings were documented and the affected data pairs were excluded.

Both the main tunnel and Sawalakot yard were considered for the study due to their meaningful difference in excavation diameter. The main tunnel's opening after excavation features a maximum dimension of 8000 mm at the cross-section, and the same for the yard equates to 16,000 mm. The I-System is applied consistently at every pull during face advancement. Arch-action time is recorded at over 100 chainages, and their associated I-Value is used to derive a correlation. **Figure 1** is a graphical representation of the polynomial correlation between I-Value and arch-action time for both the main tunnel (**Figure 1a**) and the yard (**Figure 1b**). The coefficient of determination (R^2) for each curve is shown in **Figure 1**, which represents an acceptable regression. The arch-action time, also described as bridge-action time, is defined in **Equation (2)** applicable to underground spaces:

$$t_A = \frac{1000(I)^2}{D} \quad (I) \leq 60 \tag{2}$$

where (I) is the I-Value, D is the diameter, width, or height (mm) of an underground opening (the greater value), and t_A is the arch-action time in hours.

Figure 2 is a graphical illustration of **Equation (2)** for underground spaces with D between 4000 and 16,000 mm for (I) ≤ 60. For (I) > 60, there was no concern for arch-action time considering I-Class and its support system recommendations [1]. I-Classes related to (I) > 60 represent ground–structure interaction with higher competency in stability; the same is observed when t_A is measured.

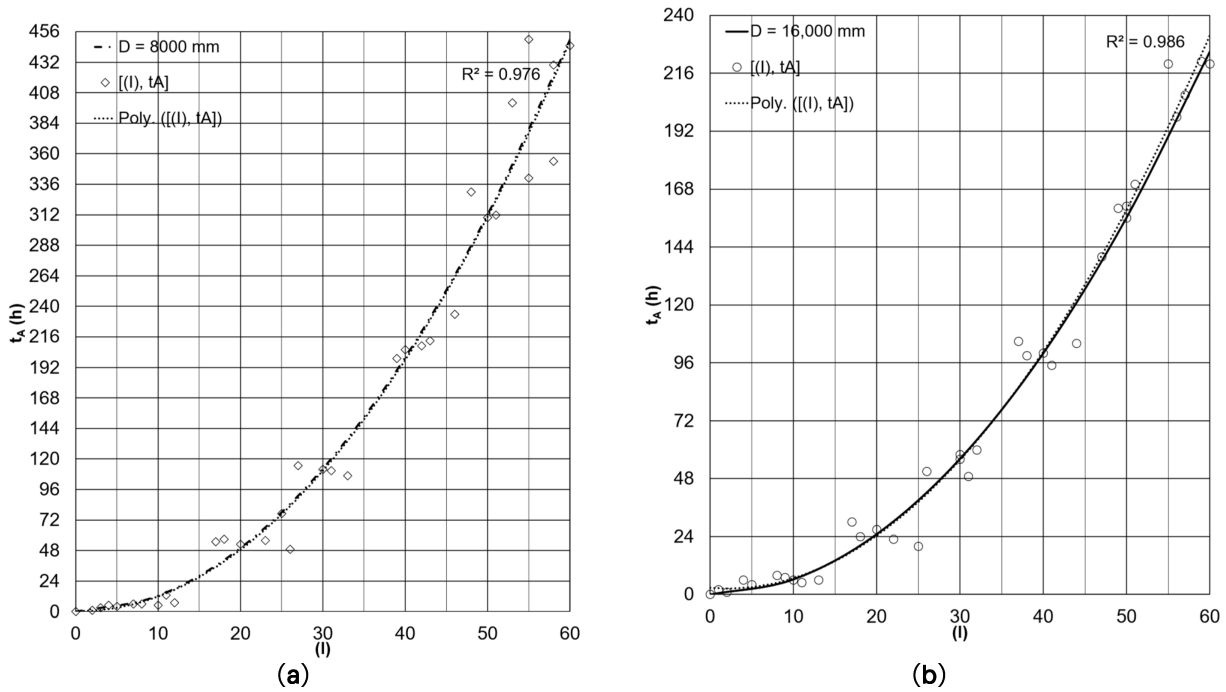


Figure 1. Polynomial correlation between (I) and t_A for tunnel T13, Jammu and Kashmir, India. Data were recorded between January 2020 and November 2023 by Amberg Engineering AG [11, 14]. T13's alignment passes through Murree's geological formation at the foreland basin of the Lesser Himalayas containing claystone, sandstone, siltstone, and mudstone from CH61013 to CH70292. T13's largest diameter (16,000 mm) is placed in mudstone at around 600 m length. (**a**) Main tunnel—T13, 8000 mm diameter. (**b**) Wider section—T13, 16,000 mm diameter. t_A: the arch-action time; (I): the I-Value; D: the diameter, width, or height (mm) of an underground opening (the greater value); R^2: the coefficient of determination.

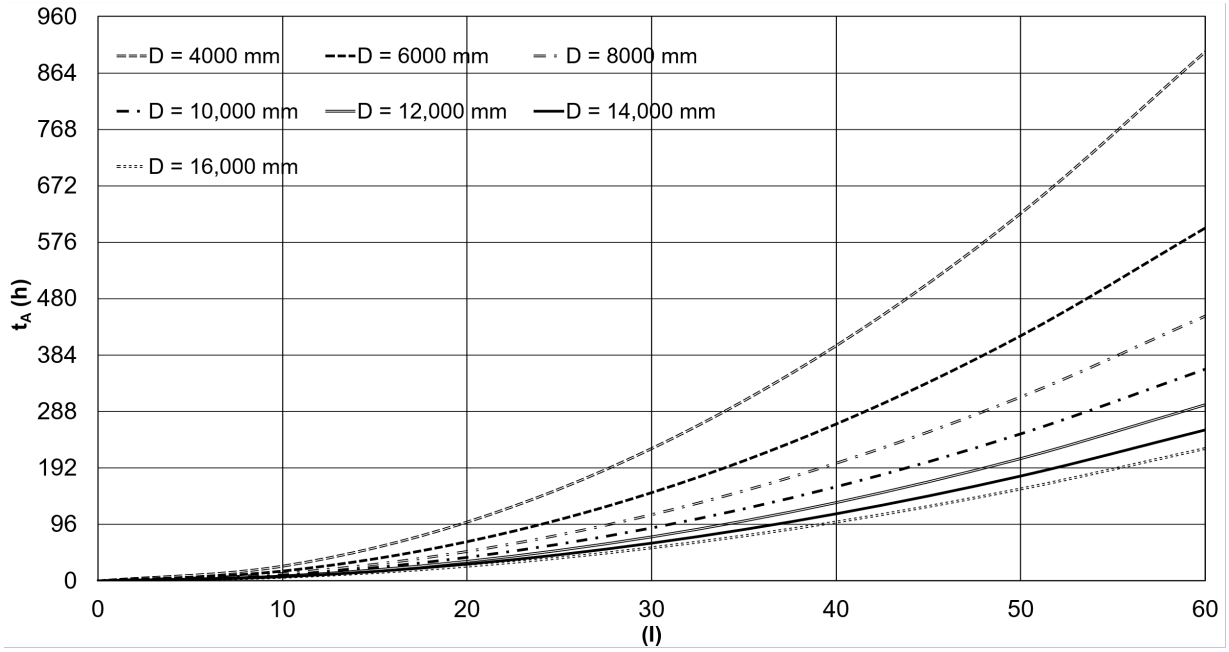


Figure 2. Graphical representation for mathematical correlation between the I-Value and arch-action time (t_A) for underground spaces with D ranges from 4000 to 16,000 mm when (I) ≤ 60. (I): the I-Value; t_A: the arch-action time; D: the diameter, width, or height (mm) of an underground opening (the greater value).

The MAE was computed for the data range illustrated in **Figure 1**. For tunnels with diameters of 8000 mm and 16,000 mm, the MAE values are 30.37 and 10.40 h, respectively, corresponding to relative errors of 6.66% and 4.69%. Taking into account the range and relative errors associated with the estimated arch-action time derived from **Equation (2)** for tunnels with diameters of 8000 mm and 16,000 mm, the mean absolute error is deemed acceptable; however, further refinement may be achieved through iterative application across additional projects.

Factors affecting the arch-action time include the ground's structural skeleton, the geological configuration, hydrogeological conditions, the ground's fabric and texture, material strength parameters, the scale of the opening, the shape of the excavation, vibration-induced damage (ViD) during excavation, dynamic forces induced by earthquake, and both virgin and in situ stress states.

Considering that all the factors influencing the arch-action time are already incorporated into the mathematical formulation of the I-System (**Equation (1)**), (I) is related to t_A with particular emphasis on the effect of the underground dimension by the inclusion of D in the proposed mathematical formulation in **Equation (2)**.

In underground works, to maintain the arch-action time, I-Class recommends immediate implementation of its recommendations, including the required support system, recommended excavation technique including pull length, partial-sequential digging and partial-sequential excavation, suggested instrumentation technique, and advised prevention technique. The immediate and appropriate implementation of I-Class recommendations is essential to control the ground–structure reaction and prevent deterioration of the arch-reaction phenomenon by inhibiting violent instability that could result in a destructive sudden collapse at the end of an enhanced failure procedure.

t_A is an important parameter to be considered in the safe design and construction of underground spaces, including tunnels, shafts, and wells. **Equation (2)** provides a plausible framework for t_A for the design of underground structures within the limitations prescribed in this study, including the range of I-Value considered in this study and the requirements for further study in different ground conditions. Further research may improve the predictive capability when applied to further cases.

3.2. Active span—underground excavations

Active span is defined as the maximum length of exposed roof, wall, and invert (full periphery) after an excavation pull in a tunnel or any other underground space, including shafts and wells, that has not yet been supported by primary measures. When primary measures are not required, the active span is assumed to be long or infinite.

The concept of an active span refers to the classes of ground that require immediate action to maintain the stability of an underground opening. This is distinct from the unsupported span defined for rock masses by Lauffer (1958) [15] as the unsupported tunnel section or the distance between the tunnel face and the nearest installed support if this is greater than the tunnel span. Lauffer's definition, which relates only to tunnel span, was later used by Bieniawski (1973) [16] in his jointed rock mass classification and cited by Hoek (2007) [17] in his developments.

The exposed span is a critical factor in the design and construction of underground works, influencing safety, ground behaviour, and construction procedures. An exposed span maintained below the maximum allowable distance provides a safe area for personnel and machinery, prevents violent and uncontrolled ground responses to excavation, and facilitates effective construction management.

The stability of an exposed span is influenced by factors including arch-action time, ground competency, the scale of the opening, the shape of the excavation, the ViD during excavation, dynamic forces, and induced stresses.

Unlike Lauffer's definition for unsupported span, the active span defined here is related to three parameters: the dimension of the underground space, the competency of the ground–structure in terms of I-Value, and the pull length of the excavation. The research has been conducted in the USBRL project in India for tunnels T01, T05, T13, and T14 for an accumulated length of approximately 46 km, including both main and escape (except T01) tunnels. It is found that this span is related to the pull length calculated using I-Value [1] (**Equation (3)**).

$$PL = 0.5D\frac{(I)}{100} \tag{3}$$

The author's research in the aforementioned tunnels [11] led to a conclusion for the active span of (I) ≤ 60 as expressed in **Equation (4)**. This is represented in an individual mathematical expression as **Equation (5)** using **Equations (3)** and **(4)**.

$$s_A = 2PL \quad (I) \leq 60 \tag{4}$$

$$s_A = D\frac{(I)}{100} \quad (I) \leq 60 \tag{5}$$

where (I) is the I-Value, D is the diameter, width, or height (mm) of underground opening (the greater value), PL is the pull length in mm, and s_A is the active span (mm).

For (I) > 60, the above research found that the active span is not a concern in the project. Consequently, the ground was competent enough to maintain the exposed span, and the arch-action time was sufficiently high. Therefore, a systematic support system was not required as a primary measure. The research thus did not establish a correlation between (I) and s_A for (I) > 60.

A sample of 5000 cases from August 2018 to May 2024 in the above research revealed that in over 90% of cases, s_A is approximately twice the value of safe PL calculated using the I-Value. This is, however, subject to some variation when the I-Value exceeds 60. No data filtering or anomaly removal has been applied to this dataset.

Figure 3 illustrates a graphical representation based on **Equation (5)** for underground spaces with D ranging from 4000 to 16,000 mm when (I) ≤ 60.

Equation (5) is an empirically derived formula based on practical experience and iterative refinement, providing a concise reference for designers, engineers and geologists to estimate the active span necessary for safe and optimised tunnelling operations. Its applicability is confined to the I-Value range established in this study and the particular ground conditions investigated. Further research across a wider range of ground types with varying competence and an expanded I-Value spectrum may enhance its accuracy.

The exposed span in underground works should be kept to a minimum—when (I) ≤ 60—to enable efficient control of ground response to excavation. Otherwise, safety is compromised, construction costs are significantly increased, and deadlines are missed due to rectification, retrofitting, or even rehabilitation required after the ground exhibits violent behaviour as a result of inaction in supporting the exposed span.

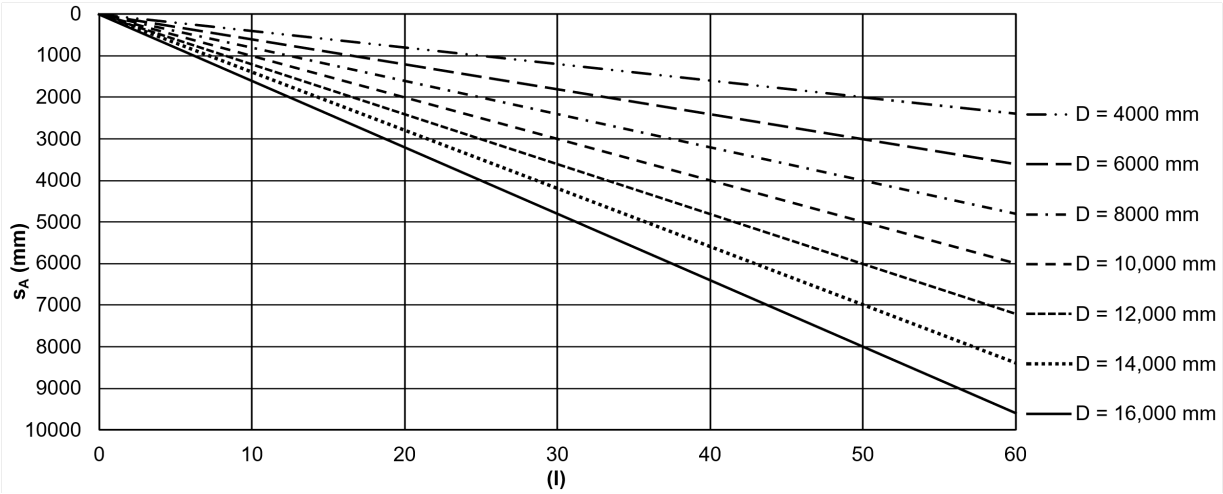


Figure 3. Graphical representation for correlation between (I) and s_A for underground spaces with D ranges from 4000 to 16,000 mm when (I) ≤ 60. Data are recorded between August 2018 and May 2024 by Amberg Engineering AG [11, 18–21]. (I): the I-Value; s_A: the active span; D: the diameter, width, or height (mm) of an underground opening (the greater value).

Conversely, maintaining and taking appropriate care of the active span will minimise required measures, ground behaviour will be controlled, associated ground hazards will be eliminated, and advancement maximised, resulting in safe and cost- and time-efficient tunnelling procedures.

3.3. Slip-action time—surface structures

Slip action is defined as the initiation of instability within a slope, which is the beginning of a failure procedure. The slip-action time is the maximum period of time between the exposure of the slope by excavation and the occurrence of the wake-up moment of the ground.

Research conducted at the critical slope of Sawalakot railway yard from February 2022 to November 2023 yielded promising results in the derivation of a relationship between slip-action time, I-Value, and slope height [11].

The global slope of the Sawalakot yard was monitored after stabilisation following a destructive global landslide in January 2022 caused by heavy rainfall. The slope's length along the railway track at the toe is approximately 150 metres. The critical slope is located at CH70336 along the alignment at the portal of the T13 in Sawalakot. The host slope consists of claystone and mudstone forming a highly jointed and fractured zone containing four joint sets and a bedding plane. The I-Value for the critical slope at Sawalakot railway yard is 21 (A_i = 0.98, C_i = 9, H_i = 3, P_i = 8.4, S_i = 9.6, DF_i = 0.85, and ET = 0.80). This represents the I-08 class with Poor ground–structure competency and High hazard/risk level as shown in **Table 1** [1].

Figure 4 illustrates the graphical details of the recorded data for I-Value and the slip-action time. The data presented in **Figure 4** comprises 135 pairs of I-Value and slip-action time following the elimination of anomalies as per the protocol provided in Section 2. The initial sample size, prior to the exclusion of anomalies, was 143. Following the identification of anomalies, the investigation confirmed that the cause of the invalid data was identical to that outlined in Section 3.1. These anomalies were documented and subsequently excluded from the data pairs. No mathematical threshold is applied to this removal, and it does not affect reproducibility. The berm width is approximately 1000 mm, and the slope height is 13,000 mm.

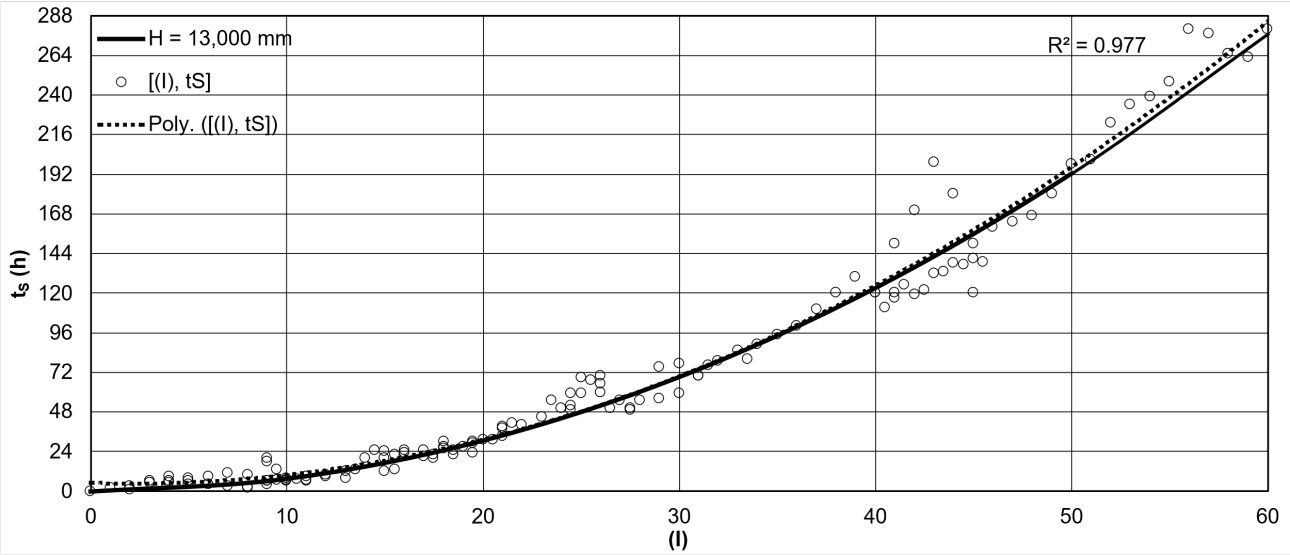


Figure 4. Polynomial correlation between (I) and t_S for tunnel Sawalakot yard's slope, Jammu and Kashmir, India. Data were recorded between February 2022 and November 2023 by Amberg Engineering AG [11, 22]. (I): the I-Value; t_S: the slip-action time; H: the height of the slope; R^2: the coefficient of determination.

The data pairs presented in **Figure 4** contain (I) ≤ 60 only, which precluded a meaningful relationship between the recorded higher I-Values and the slip-action time. Continuous 3D monitoring with fortnightly readings is carried out over a period of twenty-two months at the aforementioned slope with a global height of 40 m. The slope comprises three berms each with a local slope height exceeding 13 m.

A polynomial curve is fitted to the data and the coefficient of determination is satisfactory, as illustrated in **Figure 4**. This is defined mathematically in **Equation (6)**. Although groundwater conditions are assumed as inputs in calculating the I-Value for the slope under consideration, the observations are independent of repeated measurements and monitoring. This limits the applicability of the equation until further validation is conducted on slopes exhibiting diverse geological, geometrical, and hydrogeological characteristics.

$$t_S = \frac{B(I)^2}{H} \quad (I) \leq 60 \tag{6}$$

where (I) is the I-Value, B is the width of the berm (mm) in a slope or trench, H is the height of the slope (mm) in a local or global slope or trench, and t_S is the slip-action time in hours.

The MAE calculated for the range estimated in **Figure 4** is 14.83 h. The corresponding relative error derived from **Equation (6)** is 8.7%, which constitutes an acceptable level of accuracy for engineering prediction. This precision may be improved through further application across additional projects. This equation is restricted to the specified range of I-Values and derived from the ground conditions investigated during the research project. To broaden its scope of application and improve the accuracy of slip-action time prediction, its implementation in additional projects with different slope geometry is strongly recommended.

The slip-action time is influenced by parameters similar to those affecting the arch-action time. The interval from the exposure of a slope by excavation to the placement of a support system should be kept as low as possible to maintain the safety and health of the slope and prevent the application of additional stabilisation measures or the rectification of potential damage from violent ground behaviour.

3.4. Plastic zone—underground spaces

The plastic zone is defined as an area surrounding an underground space that develops due to permanent ground deformation after excavation. Induced stress within this region, where the ground is plastically deformed, exceeds the yield strength of the medium hosting the underground opening. Analysis of the plastic zone is essential in the design procedure for underground spaces to understand ground behaviour, associated hazards, and required mitigation measures. There are three main approaches to analyse the plastic zone surrounding underground spaces: analytical, numerical, and empirical.

Analytical methods (e.g., the method proposed by Bray, 1987 [23]) are typically limited to a specific section and shape, making them often impractical for real construction applications.

Numerical methods are widely employed in numerous research studies for the analysis of the plastic zone based on the analytical methods. They mainly include the Finite Difference Method (FDM) using Fast Lagrangian Analysis of Continua (FLAC2D/3D) [24], Distinct Element Method (DEM) using Universal Distinct Element Code (UDEC) [25], and Finite Element Method (FEM) using ABAQUS [26] or ANSYS [27]. In a 2024 study, Luo et al. [28] propose a novel numerical solution for determining the radius of the plastic zone around tunnels in non-uniform stress fields, validated through FLAC3D simulations and empirical case studies. The dimensions of the plastic zone are significantly influenced by cohesion, the angle of internal friction, and vertical stress, whereas the lateral pressure coefficient determines its geometry [28].

Empirical methods are considered practical and reliable; however, they may require further case studies for verification.

The plastic zone surrounding an underground opening may be extended to the ground surface if the depth of placement is shallow, the opening is large, an inappropriate excavation technique is employed, the ground properties are incompetent, or inapplicable support is applied. The size and shape of the plastic zone are influenced by several factors as follows:

- The ground's mechanical properties: The plastic zone expands when the ground is incompetent; the greater the I-Value, the smaller the plastic zone. When the I-Value tends to zero and an underground opening is placed at a shallow depth, the plastic zone expands excessively and may reach the ground surface. In this condition, the immediate application of recommended measures by the I-System is crucial in minimising the size and shape of the plastic zone and preventing failure. These measures also extend the arch-action time, enabling engineers to implement post-excavation stabilisation measures. Lu and Tu [29] consider the internal friction angle and cohesion as parameters that influence the range of the plastic zone.
- Excavation technique: A higher ViD leads to the formation of a larger plastic zone [1]. Conversely, at lower levels of vibration produced during excavation, less deterioration is generated; therefore, excavation results in the formation of a smaller plastic zone around the opening. Protocols for controlling ViD should be employed during excavation to minimise and control the permanently deformed zone around an underground space. Optimised energy distribution is essential in ViD when blasting is utilised for excavation [30], as it governs the extent of the plastic zone.
- Induced stresses: Higher induced stresses result in a larger plastic zone. Tunnels placed in high-stress zones have an extended plastic zone several times the tunnel diameter.
- The ratio of virgin stresses (horizontal to vertical): The ratio of in situ stresses ($\frac{\sigma_h}{\sigma_v}$), commonly referred to as the k ratio, is a key factor in defining the shape of the plastic zone. When k approaches zero, σ_h is nearly zero, resulting in a taller but narrower zone resembling a vertical oval. Conversely, when σ_h exceeds σ_v, the plastic

zone is wider but shorter, resembling a horizontal oval. The scenario is different when k equals 1, resulting in a circular plastic zone with nearly equal width and height. This ratio is influenced by numerous factors, including depth, discontinuities, water content, temperature, topographic features, surface load, tectonic stresses (active and remnant), residual stresses from magma cooling, metamorphism and metasomatism, and terrestrial stresses from seasonal variations, the moon's gravitational pull, and diurnal stresses [31].

- Shape of the excavation: The shape of an excavation plays a destructive role when inappropriately selected in the design procedure for an underground opening. For example, selecting a vertical oval for a tunnel when $\sigma_h > \sigma_v$ can lead to excessive widening of the plastic zone and large-scale lateral deformation, convergence, and/or collapse.
- The size of the excavation: This is directly related to the size of the plastic zone formed. The primary and final stability of an underground space is therefore directly related to the size of the excavation.
- The depth of placement of the underground opening: The plastic zone at greater depth is relatively larger compared to the one for medium depth of placement due to greater induced stresses. This is a different case when the depth of placement is shallow. In shallow depth, the plastic zone may be enlarged and excessively extended towards the ground surface, which may lead to serious instability. When the depth of an underground opening is shallow, there is less confinement surrounding the periphery of the space. This stress state aggravates the generation of more aggressive shear forces and consequently the occurrence of non-uniform displacements of ground fragments, which facilitates further disintegration of resting fragments after the opening is made. This condition results in large deformations leading to the extension of the plastic zone and subsequent subsidence that can be extended to the surface in more severe cases. Pre-excavation measures and immediate application of a post-excavation support system are required to control the consequences of shallow depth.
- The problematical and structural configurations of ground: Active fault zones, horsts, grabens, and foldings generate greater stress, thereby enlarging the size of the plastic zone. Tectonic stresses are considered parameters that influence the extent of the plastic zone [29].
- Implemented (mainly pre-excavation) support system: This factor is employed to control the size and shape of the plastic zone surrounding an opening. Pre-excavation measures are implemented to minimise the radius of the generated plastic zone and control its enlargement. The position and orientation of systematic bolting contribute to the minimisation and change in the shape of the plastic zone. Post-excavation support systems further prevent the enlargement of the plastic zone by the placement of rigid structures with sufficient capacity to resist deflection, thereby inhibiting further deformation.

The enlargement of the plastic zone during excavation may have several significant consequences, including a heightened risk of safety and potential hazards such as collapse. This could result in a downgraded I-Value, necessitating additional measures, increased costs for these measures, and compromised structural integrity. The consequences could also include damage to the structure, machinery, and equipment, and an extended execution cycle.

Figure 5 schematically demonstrates the plastic zone around a typical tunnel section after excavation in a temporarily stable position. In this figure, profiles for the desired section, overbreak resulting from excavation (post-excavation profile), ViD zone (within the stress-induced plastic zone), and stress-induced plastic zone are shown.

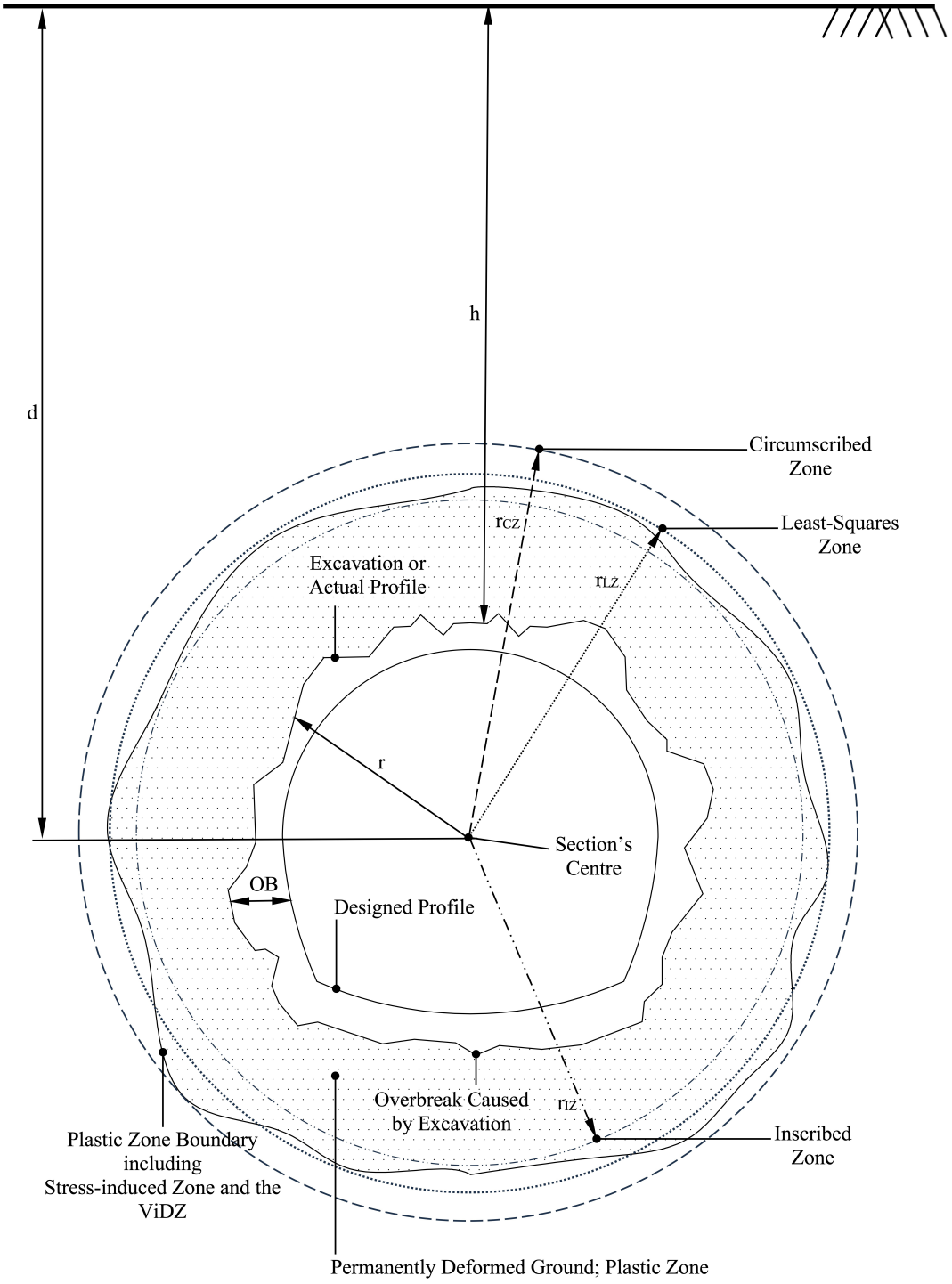


Figure 5. Illustration for the plastic zone around an underground opening with engineering simplification in assumptions. ViDZ: Vibration-induced Damage Zone; OB: Overbreak; r: the radius of the underground opening; r_{CZ}: the radius of the plastic zone (circumscribed zone) assumed around an underground opening as the worst scenario (most extensive damage) in the deterioration of ground by excavation; r_{LZ}: the radius of the plastic zone (least-squares zone) assumed around an underground opening as the medium scenario (medium degree of damage) in the deterioration of ground by excavation; r_{IZ}: the radius of the plastic zone (inscribed zone) assumed around an underground opening as the best scenario (least damage) in the deterioration of ground by excavation; d: the depth of placement of the underground opening; h: the height of overburden.

Parameters r_{CZ}, r_{LZ}, and r_{IZ} shown in **Figure 5** describe the radius of the plastic zone around an opening as the circumscribed, least-squares, and inscribed zone respectively. These areas represent different extensions of the plastic zone caused by induced stresses after excavation from the worst to the best scenario. Circular shape for the plastic zone is assumed here for the purpose of engineering simplification; however, field measurements also resulted in concluding the circular shape for this case. This may be resulted from overbreak, as the perfect horseshoe is not achieved after blasting. The plastic zone's shape is directly influenced by k.

The shape assumed in **Figure 5** for the plastic zone represents the case when k equals 1. There are many shapes associated with the plastic zone that may form around an underground opening; however, the circular shape is the most common with engineering simplification. Other common regular shapes include horizontal or vertical parabolic, oval/ellipse, and butterfly shapes.

The generation of overbreak is a significant issue in tunnelling works when inappropriate excavation techniques are employed. The cause of overbreak also influences the shape and size of the plastic zone, depending on the degree and orientation of damage induced to the surrounding ground. When excessive overbreak is observed in an underground space, it indicates an enlarged plastic zone, which requires attention to the consequences of ViD. The radius of the plastic zone may be greater than the radius of the ViD zone (ViDZ) [1]; however, in the worst-case scenario, the radius of the ViDZ equates to the radius of the stress-induced zone when inappropriate excavation techniques are employed.

The plastic zone here is defined as a circumscribed zone, which is the maximum area around an underground opening that has undergone permanent deformation after excavation. Thickness of the plastic zone is defined as the radial width of the area beyond the periphery of the opening, which has undergone permanent deformation. It is also described as a deformed band of ground surrounding the periphery. In order to clarify the parameters used in **Figure 5**, the radius of the plastic zone is defined in **Equation (7)**:

$$r_{PZ} = t_{PZ} + r \quad r = \frac{D}{2} \quad r_{PZ} \approx r_{CZ} \quad r_{CZ} > r_{LZ} > r_{IZ} \tag{7}$$

where r_{PZ} is the radius (m) of the plastic zone around an underground opening after excavation, which almost equates the radius of circumscribed zone, t_{PZ} is the thickness (m) of the plastic zone beyond the periphery of underground opening (deformed band around the periphery after excavation), r is the radius (m) of the underground opening, D is the diameter, width, or height (m) of the underground opening (the greater value), r_{CZ} is the radius (m) of the plastic zone (circumscribed zone) assumed around an underground opening as the worst scenario (most extensive damage) in the deterioration of ground by excavation, r_{LZ} is the radius (m) of the plastic zone (least-squares zone) assumed around an underground opening as the medium scenario (medium degree of damage) in the deterioration of ground by excavation, and r_{IZ} is the radius (m) of the plastic zone (inscribed zone) assumed around an underground opening as the best scenario (least damage) in the deterioration of ground by excavation.

In **Figure 5**, ViDZ is placed within the plastic zone around the periphery of the underground space formed by implementation of an excavation technique (e.g., Drill and Blast (DnB) technique). The plastic zone is generated by induced stresses as well as ViD by blasting or another excavation technique's impact.

The thickness of the plastic zone (t_{PZ}) for an underground opening after excavation in a temporarily stable condition is estimated using an empirical equation represented in mathematical form (**Equation (8)**), which is related to the radius of the underground opening, depth of placement of structure, height of overburden, and I-Value. **Equation (9)** is derived from **Equations (7)** and **(8)**.

$$t_{PZ} = \frac{rd}{(I) + d_f(d + h)} \quad 0 < (I) \leq 100 \tag{8}$$

$$r_{PZ} = \frac{rd}{(I) + d_f(d + h)} + r \quad 0 < (I) \leq 100 \tag{9}$$

where t_{PZ} is the thickness (m) of the plastic zone beyond the periphery of the underground opening, r_{PZ} is the radius (m) of the plastic zone around an underground opening after excavation, r is the radius (m) of the underground opening as $\frac{D}{2}$, d is the depth of placement (m) of the underground opening, d_f is the depth factor, which ranges from 0.1 to 1 (see **Table 2**), h is the height of overburden (m), and (I) is the I-Value.

Table 2. Depth factor for different ranges of (I).

I-Value	0 < (I) ≤ 10	10 < (I) ≤ 20	20 < (I) ≤ 30	30 < (I) ≤ 40	40 < (I) ≤ 50	50 < (I) ≤ 60	60 < (I) ≤ 70	70 < (I) ≤ 80	80 < (I) ≤ 90	90 < (I) ≤ 100
d_f	0.10	0.20	0.30	0.40	0.50	0.60	0.70	0.80	0.90	1.00

(I): I-Value, which ranges from 0 to 100. d_f: depth factor, which ranges from 0.1 to 1.

The depth factor is a parameter used to calibrate the statistical model presented in **Equation (8)**. It is intended to incorporate variables such as the radius of the underground opening, depth of placement, and overburden height, alongside the main parameter representing the ground–structure competency, I-Value. The depth factor is adjusted to align the model output with recorded data as closely as possible, thereby minimising error.

The units for the parameters in **Equations (8)** and **(9)** must be applied with precision as defined above. The output of these equations is expressed in metres; however, it may be converted to alternative units post-calculation in accordance with the prescribed specifications or requirements. They are obtained empirically between January 2020 to May 2024 during research conducted through the practice of excavation of tunnels in the USBRL project including T01, T13, and T14 [11, 14, 18, 19, 21]. The diameters of these tunnels range from 8000 to 16,000 mm. The overburden for these tunnels ranges from 0 to 650 m. The surrounding ground contains alluvium, claystone, dolomite, sandstone, scree, shale, siltstone, and slate ranging from I-10 to I-04, as per the I-System as shown in **Table 1** [1].

The Ground Conductivity Enhanced Factor (GC_{ef}) [1] is employed for the measurement of t_{PZ}. **Equation (10)** represents GC_{ef}, which is based on GCD [32]. **Equation (11)** represents GCD based on its latest edition [32].

$$GC_{ef} = \frac{GCD_e}{GCD_p} \tag{10}$$

$$GCD = \frac{V_w}{T_i\,(P_m + L_i)} \tag{11}$$

where GC_{ef}, is the Ground Conductivity Enhanced Factor [1], GCD_e is the existing GCD (post-excavation measured GCD), GCD_p is the pre-existing GCD (pre-excavation measured GCD), GCD is the Ground Conductivity Designation, V_w is the injected quantity of water (L) during T_i (measured from the initial rise in pressure until the first drop in peak), T_i is the injection period (min) for injecting V_w water (the period from initial rise in pressure until the first drop in peak), P_m is the peak head (MPa) during T_i (the measured water pressure before the first

drop in peak; the first peak), and L_i is the length of the water-injected portion (packed length) of a hole (or perforated self-drilling anchor (SDA)) in m (length of the hole to be equal or lesser than the grouted/injected length if GCD is used for post-grouting/injection assessment).

The GCD testing method is a single-stage water injection procedure in a drilled hole, wherein water pressure is increased during injection until hydraulic jacking is observed; peak pressure prior to the first drop caused by opening the inherent crack/fissure/joint/discontinuity/void is considered as hydraulic jacking. It is conducted in this research in a fully perforated SDA hole of NX size, drilled without any drilling fluid, at desired locations determined by the research programme as per the GCD testing procedure and packed for complete sealing at the collar using top/mechanical packer. An automated Unigrout system is used, comprising an agitator and a PLC (Programmable Logic Controller) hydraulic plunger featuring a least count of 0.1 L and a pressure gauge of least count of 0.1 bar.

Potable water is injected exclusively, and the resultant pressure increase is monitored. Recording of water intake and elapsed time is maintained. V_w in T_i period from the initial rise in pressure until the first drop in peak pressure is measured. Pressure during the test is recorded, and the peak pressure before a sudden drop is designated P_m. The GCD is subsequently calculated using **Equation (11)**. The procedure adheres strictly to GCD testing protocols for both GCD_e and GCD_p at each location. GC_{ef} is then computed using **Equation (10)** for the location. This value determines the depth at which conductivity is altered after excavation, thereby defining the depth at which t_{PZ} is measured. The measurement is conducted at the most critical point of the tunnel at the periphery, and the thickness of the plastic zone is determined from this measurement.

Each test on a single hole, including preparation and reporting, takes approximately 60 min. The testing requires a geologist or engineer and a technician to complete the test. A group of 159 data pairs of I-Value and t_{PZ} in tunnels with an excavation diameter of 8000 mm is screened after removing anomalies as per the protocol provided in Section 2. The initial sample size, prior to the exclusion of anomalies, was 174. The identified anomalies comprised data pairs associated with periods of Unigrout system unavailability during which an uncalibrated ordinary water pump substitute was used; measurements disrupted by power failures during testing; and drilling conducted at unauthorised locations rather than at the designated critical point. Investigation confirmed a combination of human and mechanical error, alongside non-compliance with the testing protocol. The affected data pairs were consequently excluded from the analysis as per GCD testing procedure.

A power curve is fitted to the data pairs and a satisfactory coefficient of determination is achieved. **Equation (8)** represents the best fit as per the power correlation shown in **Figure 6** for a depth of placement of 25 m. The same is examined for different depths, which are represented in **Figure 7**.

The outcomes of **Equations (8)** and **(9)** are examined practically, and satisfactory results are obtained when the measured thickness of the plastic zone is compared with the estimated ones using the proposed equations; however, analytical methods such as the one proposed by Bray (1987) [23] and simplified analysis using the FDM using FLAC2D were not employed, due to which there were no similarities between the sections of the tunnels in this research and the proposed methods.

If $t_{PZ} \geq h$, the stability of the underground opening is considered to be in a critical state. This condition indicates that deformation has occurred in the overburden column above the opening's crown. The column is extended towards the ground surface, and there is a high potential for material displacement towards the opening. This could result in collapse if the recommended measures by I-Class [1] are not implemented. Under such circumstances, stability is highly time-sensitive, and immediate implementation of pre- and post-excavation measures is necessary to prevent failure.

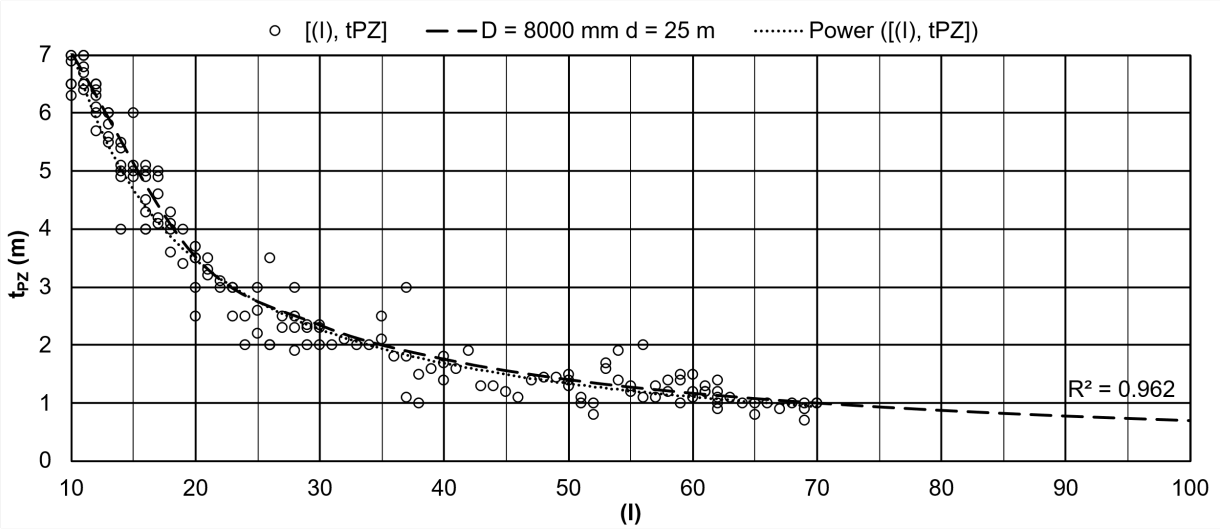


Figure 6. One hundred and fifty-nine pairs of data for I-Value versus thickness of the plastic zone around a tunnel with D = 8 m at the depth of 25 m; satisfactory power correlation with the coefficient of determination 0.962 is observed. t_{PZ} is measured using GC_{ef}. Data were recorded between January 2020 and May 2024 [11, 14, 18, 19, 21]. (I): the I-Value; t_{PZ}: the thickness of the plastic zone beyond the periphery of the underground opening; D: the diameter, width, or height of the underground opening (the greater value); GC_{ef}: the Ground Conductivity Enhanced Factor; R^2: the coefficient of determination.

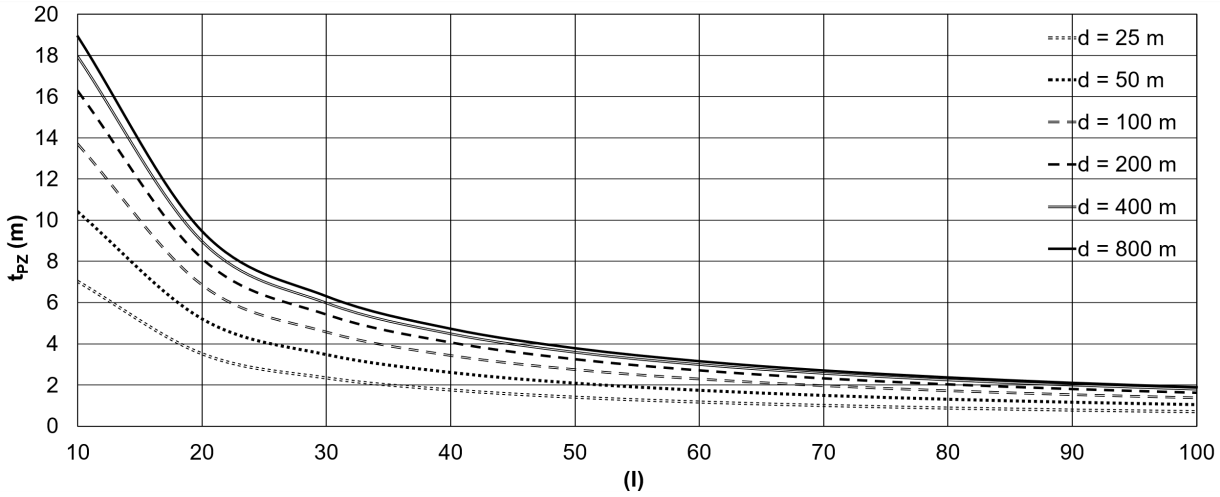


Figure 7. Graphical representation for mathematical correlation between (I) and t_{PZ} for a tunnel with D = 8 m at different depths of placement ranging from 25 to 800 m; I-Value ranges from 10 to 100. (I): the I-Value; t_{PZ}: the thickness of the plastic zone beyond the periphery of the underground opening; D: the diameter, width, or height of the underground opening (the greater value); d: the depth of placement of the underground opening.

In order to ensure prevention of further deformation at the plastic zone around an underground opening appropriately—if systematic bolting is prescribed in the associated I-Class output for the ground condition—the length of bolts should be greater than t_{PZ}. Systematic bolting with appropriate length designed after estimation of the thickness of the plastic zone is an effective measure in minimising the impact of the plastic zone and prevention of further deformation in an active mode, if applied systematically at the right position of the periphery of the underground space.

The MAE is 0.79 m, corresponding to a relative error of 13.1% calculated from the range of target values in **Figure 6** derived from **Equation (8)**. Although the coefficient of determination for the fit in **Figure 6** is 0.962, the MAE may be considered acceptable because **Equation (8)** provides only a preliminary estimate of plastic zone thickness around the underground space. It functions as a baseline model subject to iterative refinement, and the dataset in this project may contain unavoidable human error. Although **Equation (8)** is applicable across the full range of I-Values, the relative errors observed in the present project suggest that further validation is advisable for varying ground conditions, geometries, scales, and depths of placement. The accuracy of **Equation (8)** and its associated estimation error may be improved through application to additional projects.

An example for calculating the thickness of the plastic zone using **Equations (8)** and **(9)** is provided below for the following case:

An underground opening with a surrounding ground having an I-Value of 25 features a circular section of 8 m diameter with its centre placed at a depth of 150 m. The following represents the parameters derived from the above case:

- D = 8 m $\Longrightarrow$ r = 4 m;
- d = 150 m $\Longrightarrow$ h = 150 − 4 = 146 m;
- (I) = 25 $\Longrightarrow$ (From **Table 2**) d_f = 0.3.

Therefore, the thickness and radius of the plastic zone are calculated as follows by substituting the above parameters into **Equations (8)** and **(9)**:

- t_{PZ} = 5.27 m $\Longrightarrow$ r_{PZ} = 9.27 m.

3.5. Deformation limits

The aggravation of ground conditions results in the progression of the plastic zone and ultimately leads to instability. This instability may initiate with deformation or convergence if it does not cause a sudden collapse. Excessive development of the plastic zone is a consequence of faulty design or inappropriate construction activities. Contributing factors include mis-identification of ground behaviour, the use of unsuitable excavation techniques, and a failure to install a support system in a timely manner. Negligence of design principles and a dilution of quality in execution are also significant contributors.

Instrumentation and/or monitoring of the section in an underground space is a provision to check deformation/convergence, which needs to be conducted appropriately and analysed carefully. It will help to examine the condition and to evaluate the progression of the plastic zone, which results in taking required action for control of potential instabilities.

Depending on the magnitude of deformation observed, there are indications for instability and notifications for action required. Typically, there are three classes of notification issued for deformations occurring in underground spaces, including warning, alert, and alarm, that signify the level of criticality, urgency, impact, and corresponding action required.

The notification system should be established during the design procedure, and the limit of deformation for each notification should be included as well. The same system should be employed during the construction phase. These limits are related to the thickness of the plastic zone and the diameter of the underground opening in empirical equations in mathematical form presented in **Equations (12)** and **(13)** [11].

$$\delta_{Alarm} = L_m \times \frac{t_{PZ}}{10D} \quad (12)$$

$$\delta_{Alert} = \frac{\delta_{Alarm}}{2} = 0.5L_m \times \frac{t_{PZ}}{10D} \quad (13)$$

where δ_{Alarm} is an alarm limit (m) as the maximum deformation permissible for an underground opening's cross section, δ_{Alert} is an alert limit (m) for deformation occurring in an underground opening's cross section, t_{PZ} is the thickness (m) of the plastic zone beyond the periphery of the underground opening, D is the diameter, width, or height (m) of the underground opening (the greater value), and L_m is the underground space's length multiplier (m).

L_m is defined as follows considering the plane strain state:

- L_m = 1.0 m $L/D \geq 3$;
- L_m = 1.1 m $L/D < 3$.

where L is the length of underground space in relation to diameter, width, or height.

The alarm and alert limits calculated using **Equations (12)** and **(13)** are in metres regardless of the parameters' unit in the equations and represent practical estimates of the permissible deformations in an underground space, which requires attention and action including instruction and/or implementation of instruction for the prevention of ground hazards, control of ground behaviour, or rectification of deformation.

It is important to note that **Equations (12)** and **(13)** are principally empirical, due to which they are based on practical experience and correlations derived from the mathematical expression of t_{PZ}; however, they are also practical as they are obtained based on trial-and-error calibration—considering the margin for safety—and corrected in practice to their existing forms. They can be employed only for a general I-Class proposed for underground structures (I-01 to I-10) [1]. They should not be used for estimation of deformation limits for special I-Class for underground structures (I-Class related to Burst Prone behaviour (I-BP), I-Class related to Time Dependent behaviour (I-TD), and I-Class related to Visco-elasto-Plastic behaviour (I-VP)) [1]. Furthermore, they are not applicable to surface structures.

It should also be noted that the alert and alarm limits may usually be considered negligible for I-01 to I-04; otherwise, the depth of placement of the underground opening is very high (greater than 1000 m).

The ground's mechanical properties induce nearly the highest impact on potential deformations in underground openings. Therefore, when the ground quality in terms of competency is quite high (e.g., I-01 to I-04), the deformations may be considered negligible and the limits may be ignored; however, depending on the depth of placement, dimensions, and the shape of the opening, further examinations may still be needed.

The alert and alarm limits are influenced by several factors similar to those that determine the plastic zone's size and shape. These include the mechanical properties of the ground, excavation technique, and the depth of deterioration impacting the underground space. Other factors include induced and virgin stresses, the shape and size of the excavation, geological configuration, ground response to excavation, implemented support systems, and their timely installation.

Table 3 presents the deformation notification system proposed for underground spaces. This table serves as a guide to identify and differentiate the levels of criticality and urgency of deformation and/or convergence, and the required action associated with each level.

Table 3. Deformation notifications for underground spaces.

Notifications	Colour code	Criterion/ identification	Criticality/urgency level	Impact level	Action level
Warning	Yellow	Crack generation/ propagation *	Low	Low	Low priority, awareness about condition, further monitoring required
Alert	Orange	**Equation (13)** ** is applied.	Medium	Medium	Warrants attention, preparation for measures, instruction required
Alarm	Red	**Equation (12)** ** is applied.	High	High	Highest priority, implementation of measures, immediate action required

* Cracks are generated on the surface of the ground or support system (e.g., shotcrete or concrete) or existing cracks are further propagated, developed, or apertured. ** Only applicable for I-01 to I-10 as general I-Classes [1].

Assuming the inputs of the example solved at the end of Section 3.4, the following is estimated for the alert and alarm notifications as follows:

- D = 8 m and t_{PZ} = 5.27 m ⟹ **Equation (12)** ⟹ δ_{Alarm} = 0.065 m ≅ 66 mm ⟹ **Equation (13)** ⟹ δ_{Alert} ≅ 33 mm.

3.6. Support system stress

Support system stress is defined by the formula given in **Equation (14)**.

$$\sigma_{SS} = [1 - 0.01(I)]\,\gamma_g D \tag{14}$$

where (I) is the I-Value. D is the diameter, width, or height (m) of the underground opening (the greater value). γ_g is the unit weight of the ground mass (KN/m^3). σ_{SS} is the support system stress (KPa).

Equation (14), inspired by Unal's formula [33], establishes an empirical relationship between ground competency via I-Value, the unit weight of the ground, and the dimensions of the underground structure. Its reliability in estimating support system stress is confirmed through field measurements between 2018 and 2024. Throughout the entire section under this research, and across other sections beyond the scope of this study, daily optimisation was implemented following each individual face pull. This involved measuring the I-Value, calculating support system stress, and conducting analysis on the prescribed measures. It ensured adequacy as part of observational design-as-you-advance in the project.

σ_{SS} is an artificially applied active resistance stress from the support system. It counteracts in situ stresses, acts in any direction, and depends on the surrounding stress field and the ground's competency to ensure the support system is adequate to handle the stress.

Conversely, the vertical component of virgin stress (σ_v) is the total overburden pressure naturally originating from the materials above and exerted by the weight of the ground at a specific depth. This in situ stress is primarily gravity-driven, acting downwards. σ_v generates the load, while σ_{SS} handles it.

σ_{SS} is a crucial parameter for analysing underground space stability. It is used as a stability indicator in design and optimisation. Given that the I-Value ranges between 100 and 0 depending on ground competency, σ_{SS} will also vary accordingly. Assuming the Extremely Good and Extremely Poor (as shown in **Table 1**; [1]) ground conditions and substituting the I-Value into **Equation (14)** yields the calculated value of σ_{SS} as follows:

- I-01 as Extremely Good $\Longrightarrow$ (I) $\rightarrow$ 100 $\Longrightarrow \sigma_{SS} = 0$;
- I-10 as Extremely Poor $\Longrightarrow$ (I) $\rightarrow$ 0 $\Longrightarrow \sigma_{SS} = \gamma_g D$.

σ_{SS} logically ranges between zero and $\gamma_g D$ across different ground types, with the best being the most competent and the worst the least.

In these scenarios, the logic behind the requirement for a support system in an underground structure is as follows:

- A support system is unnecessary when $\sigma_{SS} = 0$.
- The maximum support system is needed to counteract and manage the stresses from the ground when $\sigma_{SS} = \gamma_g D$.

The support system measures are recommended by the I-System in its general and special I-Class [1], respectively. The proposed formula for estimating support system stress should not be used alone for squeezing-, swelling-, heaving-, and burst-prone ground conditions; instead, it should be supplemented with further assessments, like field measurements. In the literature, support system stress is commonly known as support pressure. The name for this stability parameter in this article is derived from the definitions of stress and pressure and the nature of this feature's application.

4. Discussion

Equation (2) defines an empirical polynomial correlation for the arch-action time of underground structures in relation to the I-Value and the dimension of the underground opening. The coefficient of determination from the regression analysis varies between 0.976 and 0.986 for underground opening dimensions of 8000 to 16,000 mm, which is satisfactory. The unit for the arch-action time is in hours in the derived equation; however, the equation is unbalanced in terms of units on both sides. The proposed equation may be limited to the range of the dimensions of the underground opening the study is performed on. However, its applicability may be enhanced for dimensions below and above the range defined in this research by testing on further projects. This equation assists engineers and geologists in estimating the arch-action time during construction in the excavation phase, prior to the installation of primary measures. Further assessments are recommended to ensure a safe and stable space for the underground opening. The calculated mean absolute errors for tunnels with diameters of 8000 mm and 16,000 mm are 30.37 h and 10.40 h, corresponding to relative errors of 6.66% and 4.69%, respectively, which are acceptable for underground engineering applications with a sufficient level of accuracy.

Equation (5) in this research establishes a correlation between the active span, the I-Value, and the dimension of an underground opening. This measure assists engineers and geologists in taking action in implementing the required support system for ground classes requiring immediate action for I-Values below 60. The equation is

defined based on the safe pull length in underground excavation works and follows practical experience rather than theoretical or experimental principles. Its applicability is verified for underground openings with spans or heights (the greater value) of 4000 to 16,000 mm; however, for other dimensions it requires further examination and verification. Moreover, further research could relate the active span to the same variables considered in this study using an experimental approach and correlation through regression analysis, which is not achieved in this research.

Equation (6) defines the slip-action time for surface structures with the I-Value and slope geometry parameters as variables in an empirical correlation. This correlation has a satisfactory coefficient of determination of 0.977 in a non-linear regression. While the number of inputs for this regression was sufficient to derive a reliable correlation within the scope of this study, the limited number of cases for the subject slope in the project necessitates further data to enhance the applicability of the proposed equation. The slope-action time proposed in this research enables the estimation of the initiation of instability in slopes prior to the installation of a support system. The proposed equation is applicable for I-Values below 60, which inherently requires greater attention to the stability and maintenance of the structure. The calculated MAE is 14.83 h, corresponding to 8.7% of relative error. Although these values are not ideal, they are still at an acceptable level of accuracy for engineering prediction in slope engineering.

Equation (8) represents the thickness of the plastic zone generated around an underground opening. This empirical equation has unbalanced units and is derived from 159 data pairs of I-Value and observed thickness measured using the GCD. The equation provides a satisfactory coefficient of correlation (0.962) between the measured thickness and the I-Value derived from the ground. The procedure for measuring the GCD data was labour-intensive and the derivation of the equation was time-consuming. This equation provides acceptable estimation for designers in their design or optimisation of underground structures. Further research is recommended to enhance the applicability and accuracy of the estimation using the proposed equation. **Equation (8)** is applicable for whole range of I-Values and relates the thickness of the plastic zone to the I-Value and geometrical parameters including the radius of the underground opening, the depth of placement, and the height of the overburden. A factor defined as the depth factor is also included. The depth factor is logically defined based on project experience and varies between 0.1 and 1 from the lowest to the highest value of the I-Value. The depth factor has an inverse relationship to the thickness of the plastic zone and adjusts the estimated thickness value of the plastic zone in comparison with the observed value. The calculated MAE is 0.79 m, corresponding to a relative error of 13.1%. Although this relative error is suboptimal, it offers a preliminary estimate of the plastic zone thickness surrounding the underground space. Furthermore, the error rate is comparable to that achieved by sophisticated numerical methods, such as the approach proposed by Luo et al. [28], which reports a figure of 14.6%.

Equations (12) and **(13)** are experience-based and define the notification system for underground opening deformation limits. Alongside these, the criticality impact level and action level are provided to engineers and geologists during monitoring as part of observations for tunnelling works. These equations were developed in a challenging project but their reliability may be enhanced when used in further projects.

Equation (14) is an empirical equation with balanced units that provides an estimation for support system stress as a counter-acting stress to in situ stress. It is related to the I-Value, the unit weight of the ground and the greater dimension of the opening between the height or width. This equation is meant to be applicable to the whole range of I-Values but its accuracy can be improved through further application and verification in projects.

The determination of the corresponding I-Values did not incorporate direct or indirect observations of arch-action time, active span, slip-action time, plastic zone thickness, deformation limits, or support system stress. The derivation of the I-Value from ground conditions is entirely independent of the stability indicators established in this study. The I-Value is obtained through a methodology termed I-Logging [1], and is contingent upon five indices and two impact factors encompassing approximately 27 ground parameters.

5. Conclusions

This research aimed to enhance the I-System's comprehensiveness in addressing ground engineering-related matters including investigation, design, design optimisation, and problem solving for underground and surface structures. It also aimed to integrate classification and characterisation with stability assessments to assist designers, engineers, and geologists in evaluating ground–structure interaction, identifying ground behaviour, and diagnosing associated hazards and risks, particularly under challenging conditions. This research also sought to synchronise geological, geotechnical, and geomechanical assessments between project design and execution teams, eliminating judgement dispersion, and unifying the generation of a mitigation measure as an appropriate response to ground behaviour and safety assurance. The research culminates in a novel methodology, entirely contingent upon the I-System, designed to facilitate safe and optimised ground engineering operations.

The achievement of the stated objectives required a period of approximately seven years from 2018 to 2024 during the execution of the USBRL project, a major prestigious project in the state of Jammu and Kashmir, India. Experiments and experience established the foundation of this empirical development. The research utilised I-Logging (face mapping for the I-System) and GCD testing as its input data. The author's three decades of experience in research, design, and practice guided the research to the outcome presented in this article. It was intended to define the stability indicators related to the I-Value and geometrical parameters of the opening, which were subsequently implemented. This research led to the development of the arch-action time, active span, thickness of the plastic zone, deformation limits, and support system stress for underground structures and slip-action time for surface structures as I-System-based stability indicators. The applicability and consistency of the research findings have been demonstrated within the USBRL project; however, conducting further research by implementation of the stability indicators developed herein across additional projects may confirm and enhance their suitability for diverse ground conditions and geometries.

The maximum period of time between exposure of the roof by excavation and the ground's wake-up moment in underground openings is defined as the 'arch-action time' in this research; it is also referred to as 'compressive-membrane-action time' and 'bridge-action time'. An empirical equation is developed for this indicator, which is crucial for identifying ground behaviour and controlling the stability of underground openings.

The quantification of the 'active span' in this research is defined as the maximum safe length of exposed underground excavation prior to the implementation of required support measures. This is another stability indicator that should be derived from ground–structure interaction to enable a more accurate evaluation of ground competency in self-bearing of stress. The research led to development of a generally dependable practical equation facilitating this estimation for a safe and efficient advancement in tunnelling works.

An empirical equation is also proposed in this research, providing a relatively stable estimation for the 'slip-action time' in slopes. This is the maximum period of time between the exposure of the slope by excavation and the wake-up moment of ground simulating instability. This is applicable for surface works as a stability indicator.

In this research, the estimation of the size of the plastic zone surrounding underground openings in relation to the I-Value was considered as an important indicator, which is often underestimated or overestimated through analytical and numerical approaches due to inherent limitations and inaccuracies in input data. However, some research provides more compatibility with real cases, including the outcome of this research.

This research proposed the output of an experimental approach based on practical research as an empirical equation to estimate the plastic zone's size in challenging conditions while yielding steady results, barring extreme outliers.

Deformation limits in this research are considered important indicators in assessment of the stability of underground openings. The proposed equations in this research for the 'alert and alarm limits' along with the identification criteria provide practical estimations of permissible deformations for design and construction whose reliability has been proven in the USBRL project.

The final stability indicator in this research was the 'support system stress' on underground structures that aims to estimate the adequacy of the support system in handling the stress state. This is related to the I-Value in this research as part of the integration process for the stability indicators and the I-System.

This research and its application over seven years resulted in the successful completion of the USBRL project in challenging ground conditions, including highly squeezing ground, gravity-driven conditions, visco-elastic–plastic behaviour, fully plastic ground, and liquified medium highly sensitive to vibration. While the equations are designed to derive the simplest yet plausible and consistent stability indicators, their accuracy can be enhanced by applying them to more projects and modifying the proposed equations as necessary.

Funding

This research received no external funding.

Conflict of interest

The author is an employee of Amberg Engineering AG. Amberg Engineering AG played no role in the study's conception, design, execution, or interpretation, or with the writing of this manuscript. The author declares no other financial or personal competing interests.

Data availability statement

The data supporting the findings of this publication can be made available upon request.

Publisher's note

Academia.edu Journals stays neutral regarding jurisdictional claims in published maps and institutional affiliations. All claims expressed in this article are solely those of the authors and do not necessarily represent those of their affiliated organizations, or those of the publisher, the editors, and the reviewers. Any product that may be evaluated in this article, or claim that may be made by its manufacturer, is not guaranteed or endorsed by the publisher.

Copyright

© 2026 copyright by the author. This article is an open access article distributed under the terms and conditions of the Creative Commons Attribution (CC BY) license.

References

1. Bineshian H. I-System: index of ground-structure: 2021 edition. J Eng Geol. 2021; XLVI (1): 1–50.
2. IRCM. Indian railways construction manual. New Delhi, India: Ministry of Railways, Government of India; 2023. Available from: https://www.iricen.gov.in/iricen/CodeManualNew.jsp
3. Kalouni SR, Kalouni HR. Stability evaluation of rock pillar between twin tunnels using numerical modelling. KTFT J. 2024; 4: 166–71. doi: 10.3126/ktftj.v4i1.70443
4. Erharter GH, Bar N, Hansen TF, Jain S, Marcher T. International distribution and development of rock mass classification: a review. Rock Mech Rock Eng. 2025; 58 (10): 11169–80. doi: 10.1007/s00603-024-04215-8
5. Kulkarni R, Aldonkar SS. Maintenance of tunnel on Konkan railway route—a case study on Karmali tunnel. J Emerg Technol Innov Res. 2025; 12 (12): 461–8.
6. Singh J, Mir BA. Geological traverse mapping and I-System-based rock mass evaluation for the Aryankavu-Edamon tunnel corridor, Kerala. TAI J. 2026; 15 (2): 37–49.
7. Gupta S, Khan H, Ahmed M. Innovations and site-specific solutions implemented on USBRL project. Vol. 1. New Delhi, India: The Institution of Permanent Way Engineers (IPWE), Indian Railways Institute of Civil Engineering (IRICEN); 2023. p. 73–90. Available from: https://www.iricen.gov.in/iricen/IpweSeminar.jsp
8. Bhagat P, Mehra A. Surmounting the geological complexities of Reasi Thrust (MBT) while advancement of Tunnel T01 (USBRL Project) using I-TM: index of ground-structure. Water Energy Int. 2025; A-551: 17–20.
9. Mehra A. Tunnelling through Reasi Thrust—the sequence of support system in Tunnel T01 using I-TM: index of ground-structure tunnelling method, USBRL project, J&K, India. J Eng Geol. 2026; XLIX (2): 158–75. doi: 10.64944/iseg-j49/02/13
10. Dickmann T, Krueger D, Choudhary K, Bineshian H. Use of seismic body waves to classify ground structure during tunnel excavation. In: Proceedings of the ITA-AITES World Tunnel Congress 2026 (WTC 2026): Connecting Communities Through Underground Infrastructure; 15–21 May 2026; Montréal, Canada. Boca Raton, FL, USA: CRC Press; 2026. p. 999–1006. doi: 10.1201/9781042001064-124
11. Bineshian H. Stability indicators related to I-System for tunnelling projects in complex geological formations. In: Proceedings of the International Symposium on Advances in mining, Environment, and Tunnelling (ISAMET-26); 12–14 February 2026; Nagpur, India. 2026.
12. Mahi S, Bineshian H, Gupta S, Hegde RK. An overview of the success in resolving the years-lasting problem of USBRLP's T01 tunnelling in Himalayas. MBT within the RT Zone by Employing I-System and I-TM. In: Proceedings of the International Conference on Engineering Geology and Geotechniques for Safe and Sustainable Infrastructures, EGCON 2022, Kolkata, India. Kolkata, India: Indian Society of Engineering Geology (ISEG); 2022.
13. Gupta V, Chand J, Bineshian H. A comparison between conventional and modern tunnelling method: NATM vs I-TM. In: Proceedings of the Euro-Asian Conference on Sustainable Nanotechnology, Environment, and Energy (SNEE-2024); 3–4 October 2024; Greater Mohali, India. 2026. Vol. 3420. p. 030001-1–18. doi: 10.1063/5.0334447
14. Amberg Engineering AG. Appraisal report tunnel T13. Design consultancy, site services and 3D monitoring of tunnels T6, T9, T10, T11, T12, T13, T14, T15, and T16 on Katra-Dharam section of Udhampur-Srinagar-Baramulla

new BG railway line project, J&K, India, IRCON International Ltd. and NR. Report No 10N00117-T13-P-J-001-A Rev 3. Regensdorf, Switzerland: Amberg Engineering AG; 2014.
15. Lauffer H. Gebirgsklassifizierung für den Stollenbau. Geol Bauwes. 1958; 24 (1): 46–51.
16. Bieniawski ZT. Engineering classification of jointed rock masses. Trans S Afr Inst Civ Eng. 1973; 15 (12): 335–44.
17. Hoek E. Practical rock engineering. Toronto, Canada: RocScience; 2007.
18. Amberg Engineering AG. Detailed design package for tunnel T01, tunnel design, consultancy, site services, and 3D monitoring of tunnel T01 on Katra-Dharam sections of USBRL project, USBRLP. NR and KRCL, Report: IN191003-FD-T01-MS-01. Regensdorf, Switzerland: Amberg Engineering AG; 2022.
19. Amberg Engineering AG. Method statement for tunnel T01, tunnel design consultancy, site service and 3D monitoring for construction of wider section of tunnel for a length of 85 m from km 42 + 977.50 to 43 + 062.50 in tunnel T05P1 at Reasi and extension of wider section at T41P2, providing niches for tunnels T40-T47 and stabilisation of strata at Tunnel T45P2 at Sangaldan and ancillary work on the Katra-Dharam section of the USBRL project, J&K. NR and KRCL, Report: IN191003-FD-T01-MS-01. Regensdorf, Switzerland: Amberg Engineering AG; 2022.
20. Amberg Engineering AG. Detailed design package, design report, and method statement; tunnel T05. Tunnel design consultancy, site service and 3D monitoring for construction of wider section of tunnel for a length of 85 m from km 42 + 977.50 to 43 + 062.50 in tunnel T05P1 at Reasi and extension of wider section at T41P2, providing niches for tunnels T40–T47 and stabilization of strata at tunnel T45P2 at Sangaldan and ancillary work on the Katra-Dharam section of the USBRL project, J&K, India, KRCL and NR, Report: IN191003-FLD-T05-MS-001-Rev2. Regensdorf, Switzerland: Amberg Engineering AG; 2020.
21. Amberg Engineering AG. Complete design report and method statement; tunnel T14. Tunnel design, consultancy, site services, and 3D monitoring of tunnel T14 on Katra-Dharam sections of USBRL project, J&K, India, KRCL and NR, Report: IN191007-FD-T14-MS-001-Rev1. Regensdorf, Switzerland: Amberg Engineering AG; 2020.
22. KRCL. T13P2 MT4 WS; failure of host slope—a landslide native to young Himalayan terrain. Technical note, USBRL project documents. Navi Mumbai, India: KRCL; 2022. p. 1–10.
23. Bray JW. Some applications of elastic theory. In: Brown ET, editor. Analytical and computational methods in engineering rock mechanics. London, UK: Allen & Unwin; 1987. p. 32–94.
24. Itasca Consulting Group Inc. UDEC—universal distinct element code. Version 7.0. Minneapolis, MN, USA: Itasca; 2019.
25. Itasca Consulting Group Inc. FLAC2D/3D—fast Lagrangian analysis of continua in two-dimensions. Version 9.0. Minneapolis, MN, USA: Itasca; 2023.
26. Dassault Systèmes Simulia Corp. ABAQUS Analysis user's guide. Version 6.16. Johnston, RI, USA: Dassault Systèmes Simulia Corp; 2016.
27. ANSYS Inc. Academic research mechanical, release 26.1, help system: coupled field analysis guide. Canonsburg, PA, USA: ANSYS Inc.; 2026.
28. Luo Z, Zhang R, Ren L, Zheng L, Zhang Z, Zhang Z, et al. Analytical solution and factors influencing the tunnel plastic zone under a non-uniform stress field. KSCE J Civ Eng. 2024; 28 (7): 3016–32. doi: 10.1007/s12205-024-1645-8
29. Lu Y, Tu S. Rules of distribution in a plastic zone of rocks surrounding a roadway affected by tectonic stress. Min Sci Technol. 2010; 20 (1): 47–52. doi: 10.1016/S1674-5264(09)60159-9

30. Heidari R, Noroozi M, Rafiee R, ShafieiBafti A, Derakhshani R. A hybrid numerical–evolutionary framework for optimization of underground blast design. Eng Res Express. 2026; 8 (14): 175104. doi: 10.1088/2631-8695/ae8b77
31. Komurlu E, Kesimal A, Hasanpour R. In situ horizontal stress effect on plastic zone around circular underground openings excavated in elastic zones. Geomech Eng. 2015; 8 (6): 783–99. doi: 10.12989/gae.2015.8.6.783
32. Bineshian H. GCD—ground conductivity designation—2022 edition (a testing method to quantify ground's hydraulic conductivity and solidification quality. TAI J. 2022; 11 (2): 9–13.
33. Unal E. Design guideline and roof control standards for coal mine roofs [Ph.D. thesis]. University Park, PA, USA: The Pennsylvania State University; 1983.